Hot-electron photoluminescence study of the (Ga,Mn)As diluted magnetic semiconductor

V. F. Sapega,* M. Ramsteiner, O. Brandt, L. Däweritz, and K. H. Ploog
Paul-Drude-Institut für Festkörperelektronik, Hausvogteiplatz 5–7, D-10117 Berlin, Germany
(Received 28 February 2006; published 16 June 2006)

We study the spectral shape and the magnetic field induced polarization of hot-electron photoluminescence from the diluted magnetic semiconductor (Ga,Mn)As. It is demonstrated that the holes occupy predominantly the impurity band and not the valence band as required for the Rudermann-Kittel-Kasuya-Yosida-type exchange interaction. We show that the ground state of the impurity band is split by uniaxial stress or electric fields into $F=\pm 1$ states of antiferromagnetically coupled Mn ions ($J=5/2$) and valence band holes ($J=3/2$). The polarization of the impurity band holes in a magnetic field is strongly enhanced by antiferromagnetic exchange interaction with Mn ions and saturates at a value much lower than predicted by Rudermann-Kittel-Kasuya-Yosida-like models. The temperature dependence of the hole polarization shows that the ferromagnetic and paramagnetic phases coexist in the whole temperature range below Curie temperature. This observation rather supports percolation based theories of ferromagnetism in (Ga,Mn)As diluted magnetic semiconductor.

DOI: 10.1103/PhysRevB.73.235208 PACS number(s): 78.30.Fs, 76.30.Pk, 75.50.Pp

I. INTRODUCTION

The discovery of ferromagnetism in the (Ga,Mn)As diluted magnetic semiconductor[1] (DMS) has attracted considerable attention in this material as an important candidate for modeling and realizing semiconducting spintronics devices.[2,3] The introduction of Mn in GaAs gives rise to acceptors with strong antiferromagnetic exchange between electrons of the Mn $3d^5$ shell and bound valence band hole.[4–7] The holes produced by the acceptors are believed mediate ferromagnetism. The effect of magnetic Mn ions on the transport of free carriers as well as the reverse effect of spin polarized photogenerated carriers on ferromagnetically coupled Mn $3d$ spins has been observed in several experiments.[1,8–10] These experiments suggest a mutual influence of magnetic ions and free carriers. However, in spite of a great deal of theoretical activities[11–19,28] there is no complete understanding of the origin of ferromagnetism in this material system. Most frequently, the origin of ferromagnetism in this material has been described by a mean-field Zener model based on a Rudermann-Kittel-Kasuya-Yosida-(RKKY-) type exchange interaction.[11,15] This approach implies that the Fermi surface exists, i.e., that the chemical potential lies in the valence band. Furthermore, disorder is neglected altogether. However, the observations of hopping mechanism of conductivity in transport,[20] far infrared absorption,[21] angle resolved photoemission,[22] hot electron photoluminescence (HPL),[23] and scanning tunneling microscopy[24,25] as well as theoretical studies[26] demonstrated that the holes are localized in the impurity band. In this case, the description of the ferromagnetism by the percolation of bound magnetic polarons is more appropriate, as this theory assumes that holes are pinned down with a localization length L_l in the impurity band due to disorder, which it thus includes at its most fundamental level.[27,28]

Therefore, the knowledge of the hole states (mobile or localized) and the Fermi energy are important to distinguish between different theoretical approaches. Furthermore, in view of the application of (Ga,Mn)As DMSs as spin polarized injector in spintronic devices, the important question arises about the degree of hole spin polarization as a function of sample magnetization.

In this paper, we present a study of the hole polarization in a wide range of temperatures in (Ga,Mn)As DMSs by means of hot-electron photoluminescence (HPL).[29,30] This technique has been successfully used to identify the antiferromagnetic nature of the exchange interaction between the $3d$ inner shell of the Mn ions with valence band holes in Mn-doped GaAs.[4] The HPL spectrum and its circular polarization in a magnetic field provide information on the acceptor binding energy and the polarization of holes bound to single Mn acceptors or in the acceptor impurity band. Here, our study of the HPL spectra demonstrates that the valence band holes in (Ga,Mn)As DMSs occupy predominantly the Mn acceptor impurity band even for the highest Mn concentration. They can therefore not play the role of a Fermi sea in the RKKY-like exchange interaction. Furthermore, our study of the HPL polarization indicates that random strong stress or electric fields existing in (Ga,Mn)As DMSs remove the threefold degeneracy of the $F=1$ ground state (antiferromagnetically coupled $3d^5$ electrons of Mn ions and valence band holes) and leads to two $F=0$ and $F=\pm 1$ sublevels, with the latter being the ground state. The temperature activated transition into the spin unpolarized state $F=0$ can thus determine the Curie temperature of this DMS. At low temperatures we observe an abrupt decrease of the hole polarization which we attribute to the further splitting of the $F=\pm 1$ sublevels to $F=+1$ and $F=-1$ components due to the cubic symmetry. In all (Ga,Mn)As samples studied here we find a coexistence of the ferromagnetic and the paramagnetic phase below the Curie temperature.

II. SAMPLES AND EXPERIMENT

The samples for the present study were grown by molecular-beam epitaxy on GaAs(001) substrates (semiinsulating, Si or Zn doped). Prior to the (Ga,Mn)As deposition, a GaAs buffer layer was grown at 600 °C. The substrate was then cooled to 250–300 °C for the growth of 500–1000 nm of (Ga,Mn)As. The growth rate was typically

TABLE I. Parameters of the GaAs:Mn and $Ga_{1-x}Mn_xAs$ DMS samples used in this work: Mn content x as well as paramagnetic (PM) or ferromagnetic (FM) type of magnetism and Curie temperature T_C measured by SQUID.

Sample	Mn content	Magnetic state	T_C (K)
R1	2.2×10^{-5}	PM	
R2	6.8×10^{-5}	PM	
A1	6.0×10^{-3}	PM	
B1	4.3×10^{-2}	FM	55
B2	4.0×10^{-2}	FM	35

4–10 nm/min, and the As_4/Ga beam-equivalent-pressure ratio was 25–50. Several different $Ga_{1-x}Mn_xAs$ layers with $0.006\leq x\leq0.05$ were studied. The Mn concentration was obtained from the lattice constant of the (Ga,Mn)As layer determined by high-resolution x-ray diffraction. In addition, a Mn-doped 1000 nm thick GaAs layer (5×10^{17} cm^{-3}) grown at 560 °C was used as reference sample $R1$. Superconducting-quantum-interference-device (SQUID) measurements were carried out in the temperature range from 5 to 400 K to investigate the macroscopic magnetic properties of the samples and to confirm the absence of MnAs nanoclusters. The parameters of the samples are summarized in Table I.

For excitation of HPL, we used the lines of He-Ne (632.8 nm), Kr (676.4 nm), and Ar (488 nm) ion lasers. The laser power densities focused on the sample were varied in the range from 5 to 50 W cm^{-2}. The photoluminescence (PL) spectra were dispersed either by a DILOR spectrograph and detected by a charge-coupled device array or by a Jobin-Yvon U-1000 monochromator equipped with a cooled GaAs photomultiplier. The experiments were carried out in the temperature range 4–300 K in a continuous He-flow cryostat and in magnetic fields up to 12 T, either in the backscattering Faraday or in Voigt geometry. In Faraday geometry the circular polarization of the HPL was measured using a photoelastic modulator. The degree of circular polarization was defined by the common expression $\rho_c=(I^+-I^-)/(I^++I^-)$, where I^+ and I^- are the intensities of the components of the luminescence with σ^+ and σ^- polarization, respectively.

In the Voigt geometry we measured the linearly polarized HPL under unpolarized excitation. In this case, $I_\parallel$ and $I_\perp$ denote the intensities measured for the polarization axis of the emitted light parallel or perpendicular to **B**, respectively. The degree of linear polarization was defined by $\rho_l=(I_\parallel-I_\perp)/(I_\parallel+I_\perp)$. ρ_l was measured for two orientations of the magnetic field, i.e., either $B\parallel[110]$ or $B\perp[110]$.

III. RESULTS AND DISCUSSION

A. HPL spectra

In Fig. 1 we show the HPL spectra obtained from three $Ga_{1-x}Mn_xAs$ ($2\times10^{-5}\leq x\leq0.04$) samples under excitation by a He-Ne laser ($\hbar\omega_{ex}=1.96$ eV) and at a temperature of $T=5$ K. The reference sample $R1$ shows near-band gap photoluminescence due to recombination of equilibrium photoexcited free electrons with holes bound to neutral Mn acceptors (e-A°) centered at 1.411 eV.[31] Two phonon assisted replicas of the e-A° line are marked by the arrows "1" and "2." The superimposed sharp lines centered at 1.518, 1.495, and 1.46 eV were detected in all samples studied and correspond to the band gap PL from the substrate (exciton, acceptor, and phonon assisted acceptor lines, respectively). The intensity of all substrate related PL lines strongly decreases with increasing excitation energy due to decrease of the photon penetration depth.

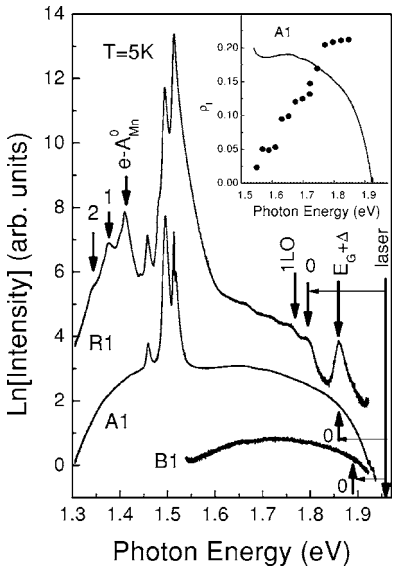

FIG. 1. HPL spectra of samples $R1$, $A1$, and $B1$ excited with $\hbar\omega_{ex}=1.96$ eV at $T=5$ K. The arrows labeled as "0" and "1LO" indicate the energy for recombination of electrons from the point of generation and after emission of one LO phonon, respectively. The recombination of equilibrium electrons with holes bound to Mn acceptor is marked by the arrow e-A°_{Mn}. Peaks labeled as "1" and "2" are the first and second LO replica of the e-A°_{Mn} band. The PL band related to the recombination of holes in the spin-orbit split-off band with the Mn double donor is labeled as $E_G+\Delta$. The inset shows the HPL spectrum (solid line) and its linear polarization (under linearly polarized excitation) for sample $A1$.

Figure 2 shows the HPL spectra of the samples $R1$, $A1$, and $B1$ obtained with excitation by a He-Cd laser ($\hbar\omega_{ex}=3.815$ eV), for which the penetration depth is smaller than the layer thickness. The high-energy tail (in each spectrum of Fig. 1), which spreads up to the laser excitation energy, is related to hot electron photoluminescence.[4] At low temperatures the HPL spectrum in acceptor doped GaAs originates from the following processes [see Fig. 3(a)].

Under cw excitation laser photons excite electrons from the heavy-hole (HH) subband into the conduction band [in the following we will discuss only this channel of excitation because of the larger density of states in this subband compared with the light-hole (LH) subband]. The electrons subsequently relax toward the Γ band minimum by emission of LO phonons in moderately doped samples or electron-hole scattering in heavily doped ones. The radiative recombination of these nonequilibrium electrons with acceptor-bound holes (A°) then leads to the HPL spectrum, which spreads

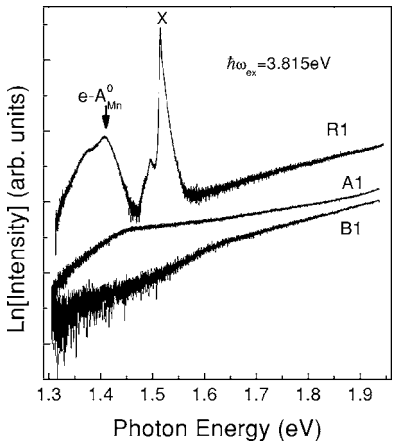

FIG. 2. HPL spectra of samples $R1$, $A1$, and $B1$ excited with $\hbar\omega_{ex}=3.815$ eV at $T=5$ K. Only sample $R1$ shows intensive and pronounced band gap PL related to the Mn acceptor e-A°_{Mn} and the acceptor bound exciton X.

from the point of creation (marked as "0" on the high energy side of the spectra) to about the bottom of the conduction band.[29,32] The electrons recombining from the bottom of the Γ point contribute to the band gap (e-A°) PL with the intensity $I \propto \tau_{nr}/\tau_r$, where τ_{nr} and τ_r are the nonradiative and radiative lifetime, respectively. The hot electron energy relaxation time is typically much shorter than the radiative recombination time (LO-phonon emission time $\tau_{LO} \sim 10^{-13}$).[32] Therefore, the HPL intensity $I \propto \tau_{LO}/\tau_r$ is generally much weaker than the band gap PL as seen in the spectrum obtained from the moderately Mn-doped sample $R1$. However, as long as $\tau_{nr} \gg \tau_{LO}$, the HPL is not affected by nonradiative recombination.

The high-energy PL tail detected in samples $A1$ and $B1$ (Fig. 1), which belong to the DMS regime, is also assigned

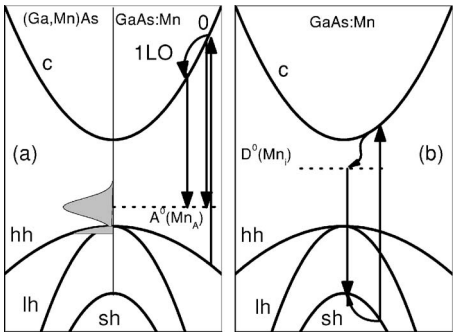

FIG. 3. (a) Schematic of HPL spectroscopy. The vertical arrow on the right shows excitation of the electrons from the heavy-hole valence band to the conduction band. The luminescence transitions from the point of creation and after emission of 1LO phonons are indicated by vertical arrows pointing down. The horizontal dashed line on the right presents monoenergetic distribution of the acceptor states in doping regime. The energy distribution of impurity band states in the DMS case is shown on the left. (b) The origin of the $E_G+\Delta$ band in GaAs:Mn. The vertical arrows pointing up and down show excitation and recombination channels, respectively. The horizontal dashed line shows the interstitial Mn double-donor state.

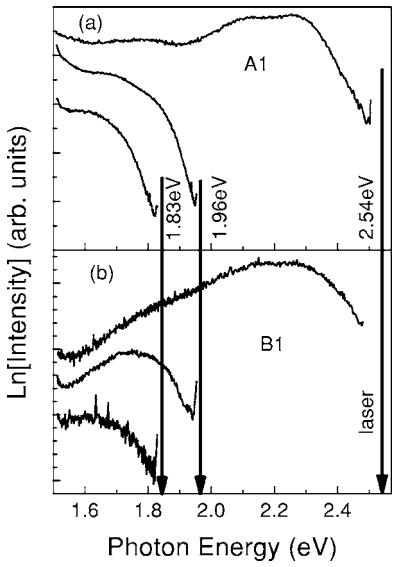

FIG. 4. HPL spectra of (Ga,Mn)As for samples of type $A1$ (a), and $B1$ (b) excited with $\hbar\omega_{ex}=1.833$ eV, $\hbar\omega_{ex}=1.96$ eV, and $\hbar\omega_{ex}=2.54$ eV at $T=77$ K. The vertical arrows indicate the energy of the exciting laser lines.

to HPL. However, in heavily doped GaAs such a PL tail can appear also due to either a Burstein-Moss-like shift of the emission to higher energies or indirect optical transitions induced by disorder in the low-temperature grown (Ga,Mn)As DMS. Our detailed study of the HPL spectra and their polarization properties rules out both of these possibilities. We found that in doped ($R1$) as well as in DMS samples ($A1$ and $B1$) the HPL is linearly/circularly polarized under linearly/circularly polarized excitation. In the onset we measured linear ($\rho_l=0.22-0.26$) and circular ($\rho_c=0.3$) polarizations of the DMS samples which are close to those observed in GaAs samples doped by Mn ($R1$) or other shallow acceptors (C, Be, Zn).[4,32] As in GaAs doped with C, Be, or Zn (Ref. 32). the linear polarization in DMS samples tends to zero when the electron kinetic energy goes to zero (see, e.g., the solid circles for sample $A1$ in the inset in Fig. 1). It was demonstrated in Ref. 33 that the linear and circular polarization of HPL is determined by the selection rules for direct interband optical transitions in III-V semiconductors. This leads to the conclusion that the HPL from these DMS samples is also related to direct transitions, and disorder-induced indirect transitions can be ruled out.

Another important signature of HPL is demonstrated in Fig. 4, which presents the HPL spectra of the two samples $A1$ and $B1$ obtained with different excitation energies ($\hbar\omega_{ex}=1.833$, 1.959, and 2.54 eV). Contrary to the PL related to the Burstein-Moss effect, where the high-energy cutoff is fixed and determined by the Fermi energy, the onset "0" of the HPL spectra shifts to higher energies with increasing excitation energy, in accordance with the scheme for the optical transitions depicted in Fig. 3(a).

The increase of the Mn content up to 1% in low-temperature grown (Ga,Mn)As strongly modifies the band gap as well as the HPL. First, instead of an intense and well defined (e-A°) PL line, the DMS samples show weak and

broad PL signals or none at all in the near band gap region (see the spectra of samples $A1$ and $B1$ in Fig. 2). The strong suppression of the band gap PL is related to nonradiative centers generated during the growth of (Ga,Mn)As under the required low-temperature conditions resulting in a nonradiative lifetime of $\tau_{nr} \sim 10^{-13}-10^{-12}$ s.[34,35] The cascade of recombination acts from the onset of the HPL down to the band edge depletes the number of electrons available for further recombination at the band edge. Quantitatively, the ratio between the intensity of two successive recombination acts is $I_{i+1}/I_i = 1/(1+\tau_{\mathrm{LO}}/\tau_{\mathrm{eff}})$ with $1/\tau_{\mathrm{eff}} = 1/\tau_r + 1/\tau_{nr}$. When τ_{eff} becomes comparable to τ_{LO}, the intensity thus drops exponentially with decreasing energy as observed experimentally for sample $B1$ in Fig. 2. The intensity ratio between the band gap PL and the first HPL peak ("0") is given by $I_{\mathrm{BE}}/I_{\mathrm{HPL}} = (\tau_{\mathrm{eff}}/\tau_{\mathrm{LO}})[1/(1+\tau_{\mathrm{LO}}/\tau_{\mathrm{eff}})]^{n-1}$ for n LO phonons relaxing from the onset "0" down to the band edge. For electrons with a kinetic energy lower than that of an LO phonon, relaxation occurs via emission of acoustic phonons and thus slows down significantly. In this case the effect of nonradiative recombination on the band gap PL is even stronger than outlined above, which explains the absence of any appreciable band gap PL for sample $B1$ in Fig. 2. These considerations clearly show that in the presence of strong nonradiative recombination the density $n(\varepsilon)$ of recombining hot electrons decreases when their kinetic energy tends to zero.

Simultaneously, the high Mn concentration in the (Ga,Mn)As DMS samples strongly modifies the HPL shape and shifts its onset to higher energies in comparison to the doping regime (see Fig. 1). Two reasons are responsible for this HPL transformation. First, in contrast to the case of electron-LO-phonon scattering characteristic for the moderately doped sample $R1$, the energy loss in DMS due to e-A° and e-HH scattering processes is not well defined. Therefore, the HPL spectrum with oscillating intensity transforms into an unstructured spectrum. Second, and more important, is the formation of an impurity band in the DMS regime. Indeed, when the Mn concentration increases, the monoenergetic Mn acceptor level spreads into an impurity band, which can even merge with the valence band [see Fig. 3(a)]. The onset of the HPL spectrum 0 on the energy scale is determined for monoenergetic acceptors by the simple expression

$$\hbar\omega_0 = \hbar\omega_{\mathrm{ex}} - E_A - \varepsilon_{HH}, \tag{1}$$

where $\hbar\omega_{\mathrm{ex}}$ is the excitation energy, E_A is the acceptor binding energy, and ε_{HH} is the kinetic energy of heavy holes determined by the dispersion of the HH band. For excitation with the He-Ne laser $\hbar\omega_{\mathrm{ex}} = 1.959$ eV we obtain ($\varepsilon_{HH} = 0.038$ eV).[30] The broadening of the acceptor level and the impurity band formation leads to a shift of the HPL onset 0 towards the excitation energy. The effective energy gap between the impurity band and the valence band can thus directly be measured. In the reference sample $R1$ with pronounced LO-phonon oscillations the estimated binding energy of the Mn acceptor is $E_A = 122$ meV,[36] which is close to the measured value of Ref. 31 and agrees with the result of our band-gap PL measurements. In the DMS samples $A1$ and $B1$ the HPL spectra are unstructured, making the determination of their onset more ambiguous. A rough estimate shows that the energy gap between the impurity band and the top of the valence band is about $\Delta \sim 0.03$ eV in the (Ga,Mn)As sample with the highest Mn concentration ($x = 0.043$).

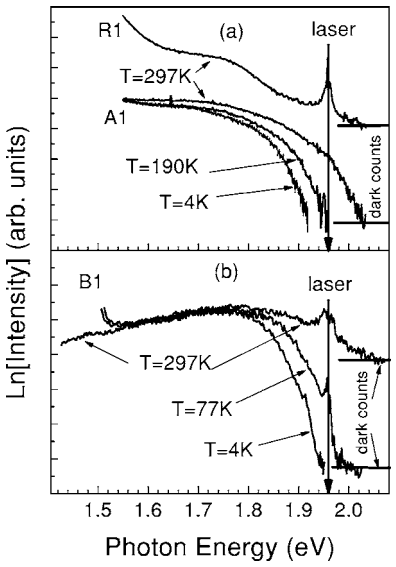

FIG. 5. HPL spectra of (Ga,Mn)As of samples $R1$ and $A1$ (a), and $B1$ (b) excited with $\hbar\omega_{\mathrm{ex}} = 1.96$ eV at three different temperatures. The vertical arrows indicate the energy position of the laser line.

The existence of a noticeable gap between the impurity band and the valence band top is also supported by our studies of the influence of the sample temperature on the HPL spectrum. At higher temperatures, free holes appear in the valence band due to thermal activation from the impurity band. The density of free holes depends on the temperature as well as on the effective energy gap between impurity and valence band. At high temperature, these holes are distributed in energy according to Maxwell's law and their kinetic energy in the valence band is $\varepsilon_{HH} \sim kT$. Therefore, electrons from the point of creation can recombine with free holes in the valence band due to vertical transitions. This channel of recombination manifests itself as a weak HPL signal near the excitation laser line. In the reference sample $R1$ with the largest acceptor binding energy, this e-HH transition appears in the HPL spectra only at room temperature (see Fig. 5). In the DMS sample $A1$ (Fig. 5) the direct e-HH transition is possible only at $T = 190$ K while in sample $B1$ [Fig. 4(b)] this transition can be detected in the HPL spectrum already at $T = 77$ K.

The analysis of the HPL spectra obtained from the reference and the DMS samples demonstrates that in a wide range of Mn concentration the valence band holes in (Ga,Mn)As are either bound to Mn acceptors or localized in the impurity band and are thus far from degeneracy as assumed in the RKKY based theory.[15] Our conclusion agrees with previous results obtained by far infrared (FIR) absorption spectroscopy from (Ga,Mn)As DMS samples ($x = 0.034$ and 0.05).[21] In this work, a broad FIR absorption peak at an energy close to the single Mn acceptor binding energy was ascribed to

transitions from the valence band to localized Mn impurity states.

The broad band centered at 1.86 eV (labeled as $E_G+\Delta$ in Fig. 1) is observed in the $R1$ sample only at near-resonant excitation with a photon energy of either 1.96 or 1.92 eV and is related to the recombination of free or donor-bound electrons with photocreated holes excited in the spin-orbit split-off valence band [see Fig. 3(b)]. This assumption is supported by the total circular polarization of this band observed under circularly polarized excitation.[37] The fact that this line shows a superlinear dependence on the excitation power density means that the recombination takes place via donors, which are partially compensated by acceptors. It is important to note that this line has never been observed in moderately or heavily acceptor doped GaAs with Zn, C, or Be.[32] Therefore we conjecture that the appearance of this band in Mn doped GaAs is due to interstitial Mn which acts as a double donor in GaAs.[38] In DMS samples this line is absent which indicates the total compensation of interstitial Mn donors in this material.

B. Polarization of HPL in a magnetic field

1. HPL polarization in Faraday geometry

The properties of HPL provide a unique possibility to study the effect of a magnetic field on the hole polarization in the impurity band. Indeed, the energy relaxation time of hot electrons is much shorter than any possible spin relaxation time. The spins of hot electrons recombining with equilibrium holes bound to an acceptor or in the impurity/valence band are therefore not oriented by the external magnetic field and do not contribute to the circular polarization of the HPL. The magnetic field induced circular polarization of the HPL is thus exclusively related to the magnetization of impurity holes.[4]

In Fig. 6(a) we present the polarization curves measured at the HPL onset for samples $R1$, $A1$, and $B1$. Note that the polarization curves do not depend on energy in the entire HPL spectral range. The solid triangles in the figure represent the magnetization curve measured for sample $R1$ and reproduce the results of Ref. 4. This dependence can be well fitted (solid line) by a model assuming that the holes bound to Mn acceptors antiferromagnetically couple with $3d^5$ electrons of the inner Mn shell.[4,39] The exchange energy, the stress induced splitting of the ground state, and the acceptor g factor, as determined in Ref. 40, amount to $\Delta=2.2$ meV, $\delta\leq 1$ meV, and $g_A=2.74$, respectively. For these parameters ($\Delta>\delta$) the theory developed in Ref. 39 predicts a saturation of the polarization at $\rho_c=0.504$. The data of Fig. 6(a) show that the transition from the doping regime (sample $R1$) to the DMS (samples $A1$-PM and $B1$-FM) is accompanied by a decrease of the saturation polarization and a decrease of the saturating magnetic field. This decrease of the hole polarization in the ferromagnetic $B1$ sample is in sharp contrast to the theoretical mean-field Zener model based on a RKKY-like exchange interaction, which predicts a hole liquid polarization up to 0.7–0.9.[15] We believe that this decrease of the polarization in a saturating field can be understood by a model assuming that the Mn acceptors (impurity band) undergo a strong effect of stress (or electric) fields, i.e., $|\delta|\gg kT, g_A\mu_B B$. On the other hand, we have demonstrated by Raman scattering[41] that the exchange energy Δ is not sensitive to the impurity band formation at least for $x\leq 0.01$. The local stress splits the ground state of the acceptors ($F=1$) in two sublevels with $F=\pm 1$ and $F=0$ projections on the stress. In this case the magnetic field dependence of the circular polarization reads[39]

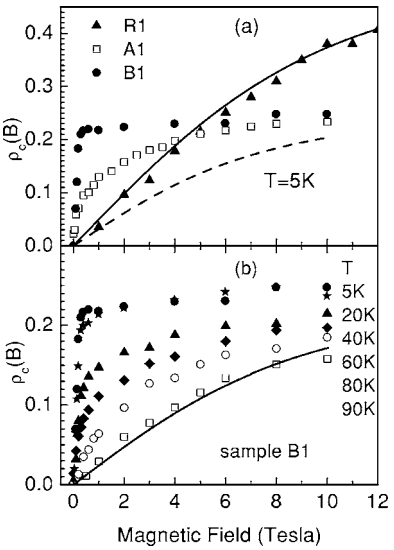

FIG. 6. Magnetic field dependencies of the HPL circular polarization: (a) measured in Faraday geometry at a temperature $T=5$ K in samples $R1$ (solid triangles), $A1$ (open squares), and $B1$ (solid circles). The solid line is a fit according to Ref. 39 for sample $R1$. The dashed line presents the expected $\rho_c(B)$ for isolated Mn acceptors in the limit of strong stress [see Eq. (2)] (b) measured in Faraday geometry at different temperatures in sample $B1$. The solid line is a fit using Eqs. (2) and (3).

$$\rho_c(B)=\frac{18}{35}\int_0^1 y\tanh\left(\frac{yg_A\mu_B B_{\text{eff}}}{kT}\right)dy, \tag{2}$$

where $y=\cos(\vartheta)$, and ϑ is the angle between magnetic field and stress direction. Expression (2) assumes an average over random orientations (spherical or cubic) of stress, and in a saturating magnetic field it gives the polarization $\rho_c(\infty)=0.257$ at $\delta>0$ and $\rho_c(\infty)=0$ at $\delta<0$. The finding that the HPL polarization in the DMS tends to the theoretical limit in a high magnetic field means that the ground state of the impurity band is formed by a stress split state with angular momentum projection $F=\pm 1$ (the $F=0$ state does not contribute to the magnetization). This assumption is supported by a recent study of the ferromagnetic resonance[42] which revealed that the cubic anisotropy fields are very large in (Ga,Mn)As (of the order of 2000 G). On the other hand, the splitting of the $F=1$ Mn acceptor state can also be induced by the strong electric field of ionized Mn acceptors or donors.

The polarization curves of the paramagnetic ($A1$) as well as the ferromagnetic ($B1$) samples differ from that predicted by Eq. (2) [see dashed line in Fig. 6(a) plotted for $B_{\text{eff}}=B$ and

$T=5$ K]. For sample $B1$ [see Fig. 6(b)] we can distinguish two magnetic field regimes in the temperature range $T=5-60$ K. First, a very fast HPL polarization increase at $B=0-0.5$ T is observed and then the polarization slows down and tends to the theoretical limit at fields higher than $B=10$ T. Such a behavior of the polarization indicates that the ferromagnetic sample is microscopically not uniform (see discussion below) and contains paramagnetic regions (slow polarization) as well as ferromagnetic regions (fast polarization). An increase of the sample temperature destroys the ferromagnetic phase and thus increases the contribution of the paramagnetic phase to the observed HPL polarization. At temperatures above 90 K the magnetic field dependence of the polarization can be well approximated by Eq. (2) with an effective magnetic field B_{eff} [see solid line in Fig. 6(a)] which is the sum of the external field (B) and the exchange field induced by the Mn ions

$$B_{\text{eff}} = B + \frac{N_0 \beta x S}{g_A \mu_B} B_{5/2}\left(\frac{g\mu_B SB}{kT}\right), \tag{3}$$

where $g=2$ is the g factor of the Mn ion, $N_0\beta$ is the p-d exchange constant, x is the Mn concentration, and $B_S(B,T)$ is the Brillouin function. At low temperatures ($T \leq 50$ K) the polarization in a magnetic field tends to saturate much faster than one can expect for the effective field given by Eq. (3). Note, however, that even in the paramagnetic sample $A1$ the polarization [see Fig. 6(a)] shows a more complicated behavior than that expected for B_{eff} given by Eq. (3). This means that the Zeeman splitting of the impurity band at low temperatures is enhanced by the ferromagnetic ordering of the Mn ions. The effective magnetic field acting on the impurity band in the ferromagnetic phase is much stronger than the external field and is proportional to the sample magnetization $B_{\text{eff}}=\lambda M(B,T)$, where λ is the Weiss constant and $M(B,T)$ is the sample magnetization. The magnetization of the sample in the direction of magnetic field (applied perpendicular to the sample layer) is proportional to the spontaneous magnetization, whose easy axis in (Ga,Mn)As lies in the layer plane.[1,10,42] Therefore, the circular polarization $\rho_c(B)$ in the low field limit can be represented as

$$\rho_c(B) \propto \rho_c^s \frac{g\mu_B \lambda M(B,T)}{kT} = \rho_c^s \frac{g\mu_B \lambda M_s^2(T) B}{2K_u kT}, \tag{4}$$

where M_s is the spontaneous magnetization, $\rho_c^s = 18/35$, and K_u is the in-plane uniaxial anisotropy constant.

The temperature dependence of the spontaneous magnetization $M_s(T)$ and the Curie temperature of the ferromagnetic transition can be determined from the field dependence of the circular polarization presented in Fig. 6(a) for different temperatures. In the high temperature limit the series expansion of Eq. (2) together with Eq. (3) or (4) gives three different types of behavior of the $T[d\rho(B)/dB]_T$ value (polarization rate) on temperature as shown in Fig. 7. For single Mn acceptors (doping regime) the value $T[d\rho(B)/dB]_T = \text{const}$ does not depend on temperature in an external magnetic field (see dotted line in Fig. 7). In the paramagnetic phase of DMS the impurity band polarization is given by the double Brillouin function [Eqs. (2) and (3)], therefore $T[d\rho(B)/dB]_T \propto 1/T$

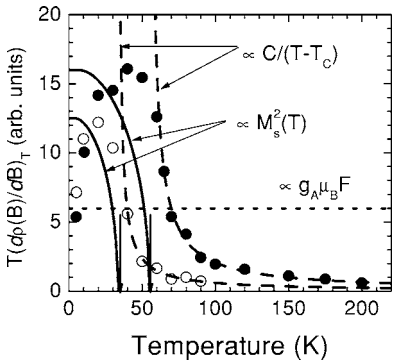

FIG. 7. Temperature dependence of the polarization rate $T(d\rho(B)/dB)_T$ for the two ferromagnetic samples $B2$ (open circles, $T_C=35$ K) and $B1$ (solid circles, $T_C=55$ K). The dashed lines represent the fit of $Td\rho/dB$ for samples $B2$ and $B1$ in the paramagnetic phase, while the solid lines show the expected behavior of $T(d\rho(B)/dB)_T$ in the ferromagnetic phase using a simple mean-field approximation. The dotted line corresponds to single Mn acceptors.

(dashed lines in Fig. 7). In the ferromagnetic phase we find $T[d\rho(B)/dB]_T \propto M_s(T)^2/K_u(T)$ in accordance with Eq. (4). The solid line in Fig. 7 represents the square of the spontaneous magnetization calculated in the frame of a simple mean field model using the Brillouin function with $S=5/2$. The solid and open circles in Fig. 7 show the dependence of the polarization rate $T[d\rho(B)/dB]_T$ on temperature for the ferromagnetic samples $B1$ and $B2$. The magnetization curves of both samples show clearly the transition from the ferromagnetic to the paramagnetic phase at the Curie temperature marked by arrows in Fig. 7.

Above the Curie temperature the value of $T[d\rho(B)/dB]_T$ is proportional to the paramagnetic magnetization (M) of the sample and thus follows the Curie-Weiss law $T[d\rho(B)/dB]_T \propto M \propto C/(T-T_C)$ (dashed curves in Fig. 7). The Curie temperatures determined by the fit of the sample magnetization in the paramagnetic phase are in good agreement with those measured by SQUID. Below the Curie temperature one would expect a saturation of the spontaneous magnetization with decreasing temperature, as illustrated by the solid curve obtained in a simple mean field model. Contrary to this expectation the spontaneous magnetization shows an abrupt decrease at temperatures below 10 K. This polarization decrease can be related to the transition into an antiferromagnetic state of some neighboring Mn ions. Such an antiferromagnetic ordering could lead to the decrease of the total magnetization of the sample, which, however, was not observed in our SQUID measurements. Therefore we conjecture that the polarization decrease at $T \leq 10$ K is induced by a splitting of the $F=\pm 1$ state. The cubic symmetry indeed removes the twofold degeneracy of the ground $F=1$ impurity band state. This effect could manifest itself in the polarization as an effective temperature increase at $T \leq \delta_4$ and $g_A\mu_B B \ll \delta_4$, where δ_4 is the splitting of the $F=1$ state in two sublevels.[39] Contrary to the holes localized in the impurity band, the monotonic saturation of spin polarization with temperature decrease was predicted for free holes in the whole temperatures range below T_C.[28]

A careful analysis of the magnetization curves measured at various temperatures on different ferromagnetic samples

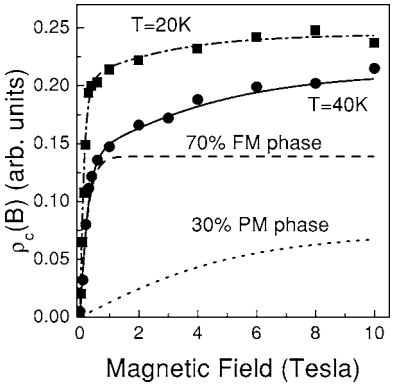

FIG. 8. Fit of magnetic field dependencies of the HPL circular polarization measured in Faraday geometry in the two-phase model for samples $B1$. The fits of the data of sample $B1$ for $T=20$ K (solid squares) and $T=40$ K are presented by dash-dotted and solid lines, respectively. The fit for $T=40$ K (solid line) is deconvoluted on paramagnetic and ferromagnetic phases, presented by dotted and dashed lines, respectively.

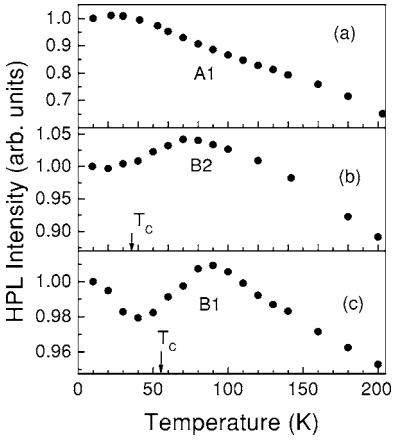

FIG. 9. Temperature dependence of the HPL intensity of samples $A1$ (a), $B2$ (b), and $B1$ (c) measured at an energy of 1.77 eV and under excitation with $\hbar\omega_{ex}=1.96$ eV. The vertical arrows indicate the Curie temperature T_C measured by SQUID.

[see Fig. 6(b) for sample $B1$] leads to the important conclusion that the ferromagnetic and the paramagnetic phases coexist below the Curie temperature as they do in the polaron-percolation theory.[28] To support this conclusion we fit the experimental polarization curves using a two-phase model. In this model we assume that the magnetic field dependence of the HPL polarization for both the ferromagnetic and the paramagnetic phases is given by Eq. (2). In this expression the temperature dependence of the effective magnetic field acting on holes is represented by Eq. (3) for the paramagnetic phase. In the ferromagnetic phase the temperature dependence of the effective field comes through the temperature dependence of the spontaneous magnetization of the sample $[B_{\text{eff}}=\lambda M(B,T)=\lambda M_s^2(T)B/2K_u]$, which is represented for sample $B1$ by the solid line in Fig. 7. With these assumptions the magnetic field dependence of the HPL polarization on temperature can be represented in the following form:

$$\rho(B,T) = \nu(T)\rho^{\text{PM}}(B,T) + [1-\nu(T)]\rho^{\text{FM}}(B,T), \qquad (5)$$

where $\rho^{\text{PM}}(B,T)$ and $\rho^{\text{FM}}(B,T)$ are the polarization of the paramagnetic and ferromagnetic phases of the sample, and $\nu(T)$ and $[1-\nu(T)]$ are the fraction of the paramagnetic and the ferromagnetic phases, respectively.

The result of this fit for $T=40$ K is shown in Fig. 8 by the solid line. The best fit for this temperature is achieved for a mixture of 30% paramagnetic (dotted line in Fig. 8) and 70% ferromagnetic (dashed line in Fig. 8) phases. The contribution of the FM and PM phases varies with temperature. The best fit for $T=20$ K (shown by the dash-dotted line in Fig. 8) is obtained for $\nu=0.15$. In this simple two-phase model we have assumed that the entire ferromagnetic phase can be described by a fixed Curie temperature of $T_C=55$ K. However, in real DMS samples the situation is more complex because the volume occupied by Mn ions and their density as well as its T_C is not well defined in the ferromagnetic phase. Therefore, the fit of the polarization curve can be improved by taking into account the real distribution of these parameters. Nevertheless, even this simple model unambiguously demonstrates the coexistence of different magnetic phases in (Ga,Mn)As DMS.

This finding is furthermore supported by the temperature dependence of the HPL intensity as shown in Fig. 9 for the paramagnetic ($A1$) and two ferromagnetic ($B1$) and ($B2$) DMS samples. The HPL intensity decreases monotonically with temperature increase for sample $A1$, while a nonmonotonic behavior is observed for samples $B1$ and $B2$. For sample $A1$, the monotonous decrease of the HPL intensity with temperature increase is related to the excitation of holes from the impurity band into the valence band. In contrast, the two ferromagnetic samples exhibit a pronounced maximum at a temperature exceeding the Curie temperature (marked by arrows in Fig. 9) with a subsequent intensity decrease. This behavior can be understood in the frame of the polaron-percolation theory.[27,28] At zero temperature, the infinite cluster formed by overlapping bound magnetic polarons occupies the entire volume for ferromagnetic samples. With increasing temperature the fraction of the volume occupied by the infinite cluster decreases to zero at $T=T_C$, while the fractions of finite clusters and isolated localized states increase with temperature. Both of these latter states are predicted to coexist at temperatures exceeding T_C. Holes localized in finite clusters experience strong exchange and Coulomb interaction with the surrounding Mn ions. The radiative recombination of holes in these clusters is less probable compared to that of holes in isolated states, because recombining electrons experience a repulsive potential from the negatively charged Mn ions surrounding the hole. Thus, the maximum in the HPL intensity is caused by the thermal excitation of holes from clusters to isolated states in the impurity band which possess a higher radiative rate. At even higher temperatures, the HPL intensity decreases as now holes are thermally excited from all states into the valence band. The fact that the maximum of the HPL intensity is reached for temperatures far exceeding the Curie temperature signifies that a significant volume fraction of the sample is occupied by finite clusters, in agreement with the prediction in Ref. 28.

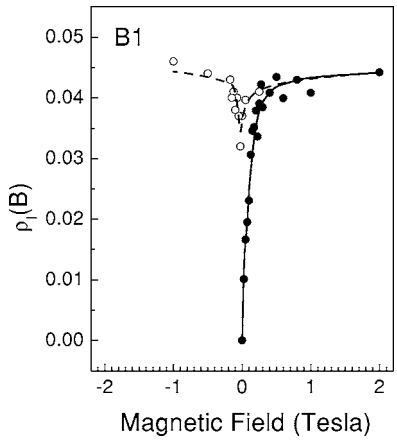

FIG. 10. HPL linear polarization measured in Voigt geometry at a temperature $T=5$ K in sample $B1$ for an up-sweep (solid circles) and down-sweep (open circles) of the external magnetic field.

2. HPL polarization in Voigt geometry

It was found in previous studies (see, e.g., Refs. 1 and 42), that the magnetic easy axis in (Ga,Mn)As grown on GaAs(001) substrates lies in the plane of the layer. A similar behavior of magnetization was found in our FM samples, which is demonstrated by the hysteresis loops in SQUID measurements in $B\|[110]$ geometry. For studying the in-plane magnetization, the Voigt geometry is the appropriate magneto-optical configuration. In this geometry, the degree of linear polarization is a measure for the orientation of Zeeman orbits with respect to the quantization (reference) axis defined by the external magnetic field. In our case, the HPL measured perpendicular to the sample plane is linearly polarized either parallel or perpendicular to the external magnetic field.

The measurements in Faraday geometry (see Fig. 6) revealed that the HPL polarization in sample $B1$ follows the magnetization curve $[B_{\text{eff}}=\lambda M(B,T)]$ at low temperatures. Consequently, we expect to observe the hysteresis behavior of the magnetization in Voigt geometry, since now the easy axis of magnetization and the external magnetic field lie in the same plane (in contrast to the measurements in Faraday geometry). Please note that the sign of the linear polarization is not expected to change when the direction of the magnetic field is reversed. The absolute value of the linear polarization, in general, differs from that of the circular polarization observed in Faraday geometry.

Figure 10 shows the dependence of the HPL linear polarization on a magnetic field in $B\|[110]$ geometry for sample $B1$. As expected, the HPL polarization for the up-sweep of the magnetic field (solid circles) resembles the magnetization curve of the virgin sample (cooled down without external magnetic field) starting with zero polarization. After the down-sweep of the magnetic field, a finite HPL polarization remains at zero magnetic field. The finite zero-field polarization corresponds to the remanent magnetization and reveals the expected hysteresis behavior. This observation evidences that the HPL polarization in the FM sample $B1$ is indeed governed by the magnetization with the easy axis lying the sample plane.

IV. CONCLUSIONS

In this paper we have studied the polarization of the HPL spectra of paramagnetic and ferromagnetic (Ga,Mn)As alloys grown on GaAs substrates by low-temperature MBE. We demonstrated that, even for layers with high Mn content, the holes occupy predominantly the impurity band and not the valence band as required for the RKKY-like exchange interaction.

Our results have shown, further, that the ground $F=1$ state of the Mn acceptors undergoes a strong random stress or electric field induced splitting into unpolarized $F=0$ and polarized $F=\pm 1$ states, the latter being the ground state of the impurity band. The cubic symmetry removes further the twofold degeneracy of the $F=\pm 1$ state. The temperature activated transition from the ground state $F=\pm 1$ into the unpolarized state ($F=0$) can thus determine the Curie temperature in the model based on carrier-mediated ferromagnetism in (Ga,Mn)As.

It is found that FM and PM phases contribute to the HPL polarization in the whole temperature range below T_C in all ($x\sim 0.008-0.043$) samples studied. This means that (Ga,Mn)As is microscopically not uniform and contains paramagnetic as well as ferromagnetic regions. The ferromagnetic and paramagnetic phases are found to coexist below T_C even in the nominally ferromagnetic samples. In the ferromagnetic sample the contribution of FM in the HPL polarization dominates only at very low temperatures when the ferromagnetic phase spreads over all the sample. This observation supports percolation based theories of ferromagnetism in (Ga,Mn)As DMS.

ACKNOWLEDGMENTS

We thank M. Moreno and C. Herrmann for sample growth, as well as G. Paris for valuable technical assistance. One of us (V.F.S.) acknowledges the financial support from the Paul-Drude-Institute and the Russian Foundation for Basic Research Grant No. 06-02-16245.

*Electronic address: sapega@dnm.ioffe.rssi.ru; Permanent address: Ioffe Physico-Technical Institute, Russian Academy of Sciences, 194021 St. Petersburg, Russia.

[1] H. Ohno, A. Shen, F. Matsukura, A. Oiwa, A. Endo, S. Katsumoto, and Y. Iey, Appl. Phys. Lett. **69**, 363 (1996).

[2] G. Prinz, Science **282**, 1660 (1998).

[3] S. A. Wolf, D. D. Awschalom, R. A. Buhrman, J. M. Daughton, S. von Molnár, M. L. Roukes, A. Y. Chtchelkanova, and D. M. Treger, Science **294**, 1488 (2001).

[4] I. Ya. Karlik, I. A. Merkulov, D. N. Mirlin, L. P. Nikitin, V. I.

Perel', and V. F. Sapega, Fiz. Tverd. Tela (Leningrad) **24**, 3550 (1982) [Sov. Phys. Solid State **24**, 2022 (1982)].
[5] J. Schneider, U. Kaufmann, W. Wilkening, M. Baeumler, and F. Köhl, Phys. Rev. Lett. **59**, 240 (1987).
[6] M. Linnarsson, E. Janzén, B. Monemar, M. Kleverman, and A. Thilderkvist, Phys. Rev. B **55**, 6938 (1997).
[7] V. F. Sapega, T. Ruf, and M. Cardona, Solid State Commun. **114**, 573 (2000).
[8] H. Ohno, D. Chiba, F. Matsukura, T. Omiya, E. Abe, T. Dietl, Y. Ohno, and K. Ohtani, Nature (London) **408**, 944 (2000).
[9] A. Oiwa, Y. Mitsumori, R. Moriya, T. Slupinski, and H. Munekata, Phys. Rev. Lett. **88**, 137202 (2002).
[10] H. X. Tang, R. K. Kawakami, D. D. Awschalom, and M. L. Roukes, Phys. Rev. Lett. **90**, 107201 (2003).
[11] F. Matsukura, H. Ohno, A. Shen, and Y. Sugawara, Phys. Rev. B **57**, R2037 (1998).
[12] H. Akai, Phys. Rev. Lett. **81**, 3002 (1998).
[13] J. König, H.-H. Lin, and A. H. MacDonald, Phys. Rev. Lett. **84**, 5628 (2000).
[14] J. Inoue, S. Nonoyama, and H. Itoh, Phys. Rev. Lett. **85**, 4610 (2000).
[15] T. Dietl, H. Ohno, and F. Matsukura, Phys. Rev. B **63**, 195205 (2001).
[16] V. I. Litvinov and V. K. Dugaev, Phys. Rev. Lett. **86**, 5593 (2001).
[17] S. Sanvito, P. Ordejón, and N. A. Hill, Phys. Rev. B **63**, 165206 (2001).
[18] C. Timm, F. Schäfer, and F. von Oppen, Phys. Rev. Lett. **89**, 137201 (2002).
[19] P. Mahadevan, A. Zunger, and D. D. Sarma, Phys. Rev. Lett. **93**, 177201 (2004).
[20] A. Van Esch, L. Van Bockstal, J. De Boeck, G. Verbanck, A. S. van Steenbergen, P. J. Wellmann, B. Grietens, R. Bogaerts, F. Herlach, and G. Borghs, Phys. Rev. B **56**, 13103 (1997).
[21] Ya. Nagai, T. Kunimoto, K. Nagasaka, H. Nojiri, M. Motokawa, F. Matsukura, T. Dietl, and H. Ohno, Jpn. J. Appl. Phys. **40**, 6231 (2001).
[22] J. Okabayashi, A. Kimura, O. Rader, T. Mizokawa, A. Fujimori, T. Hayashi, and M. Tanaka, Phys. Rev. B **64**, 125304 (2001).
[23] V. F. Sapega, M. Moreno, M. Ramsteiner, L. Däweritz, and K. Ploog, Phys. Rev. Lett. **94**, 137401 (2005).
[24] G. Mahieu, P. Condette, B. Grandidier, J. P. Nys, G. Allan, D. Stievenard, P. Ebert, H. Shimizu, and M. Tanaka, Appl. Phys. Lett. **82**, 712 (2003).
[25] A. M. Yakunin, A. Yu. Silov, P. M. Koenraad, J. -M. Tang, M. E. Flatté, W. Van Roy, J. De Boeck, and J. H. Wolter, Phys. Rev. Lett. **95**, 256402 (2005).
[26] G. A. Fiete, G. Zaránd, and K. Damle, Phys. Rev. Lett. **91**, 097202 (2003).
[27] A. Kaminski and S. Das Sarma, Phys. Rev. Lett. **88**, 247202 (2002).
[28] S. Das Sarma, E. H. Hwang, and A. Kaminski, Phys. Rev. B **67**, 155201 (2003).
[29] D. N. Mirlin, Ya. Karlik, L. P. Nikitin, I. I. Reshina, and V. F. Sapega, Solid State Commun. **37**, 757 (1981).
[30] G. Fasol, W. Hackenberg, H. P. Hughes, K. Ploog, E. Bauser, and H. Kano, Phys. Rev. B **41**, 1461 (1990).
[31] W. Schairer and M. Schmidt, Phys. Rev. B **10**, 2501 (1974).
[32] M. A. Alekseev, I. Ya Karlik, D. N. Mirlin, and V. F. Sapega, Fiz. Tekh. Poluprovodn. (S.-Peterburg) **23**, 761 (1989) [Sov. Phys. Semicond. **23**, 479 (1989)].
[33] V. D. Dymnikov, M. I. Dyakonov, and V. I. Perel', Zh. Eksp. Teor. Fiz. **71**, 2373 (1976) [Sov. Phys. JETP **44**, 1252 (1976)].
[34] M. Haiml, U. Siegner, F. Morier-Genoud, U. Keller, M. Luysberg, P. Specht, and E. R. Weber, Appl. Phys. Lett. **74**, 1269 (1999).
[35] H. Němec, A. Pashkin, P. Kužel, M. Khazan, S. Schnüll, and I. Wilke, J. Appl. Phys. **90**, 1303 (2001).
[36] I. A. Merkulov, Fiz. Tekh. Poluprovodn. (S.-Peterburg) **25**, 351 (1977) [Sov. Phys. Semicond. **25**, 214 (1991)].
[37] M. A. Alekseev, V. D. Dymnikov, D. N. Mirlin, I. I. Reshina, and V. F. Sapega, Fiz. Tverd. Tela (Leningrad) **28**, 793 (1986) [Sov. Phys. Solid State **28**, 441 (1986)].
[38] K. M. Yu, W. Walukiewicz, T. Wojtowicz, I. Kuryliszyn, X. Liu, Y. Sasaki, and J. K. Furdyna, Phys. Rev. B **65**, 201303(R) (2002).
[39] N. S. Averkiev, A. A. Gutkin, E. B. Osipov, and M. A. Reshchikov, Fiz. Tverd. Tela (Leningrad) **30**, 765 (1988) [Sov. Phys. Solid State **30**, 438 (1988)].
[40] V. F. Sapega, T. Ruf, and M. Cardona, Phys. Status Solidi B **226**, 339 (2001).
[41] V. F. Sapega, M. Moreno, M. Ramsteiner, L. Däweritz, and K. Ploog, Phys. Rev. B **66**, 075217 (2002).
[42] X. Liu, Y. Sasaki, and J. K. Furdyna, Phys. Rev. B **67**, 205204 (2003).